IMPROVEMENTS IN HEAT TRANSFER NETWORK MODELLING FOR OIL-COOLED POWER TRANSFORMER WINDINGS

Coddé J.* and Baelmans M.
* Author for correspondence
Department of Mechanical Engineering,
University of Leuven,
Leuven, 3001,
Belgium,
E-mail: Joris.codde@kuleuven.be

Wim Van der Veken
CG Power Systems Belgium NV
Mechelen, 2800,
Belgium

ABSTRACT

In this paper accurate modelling of heat transfer from power transformer winding conductors to cooling oil is envisaged. To this end the network model of Radakovic & Sorgic [1] is validated against more detailed CFD simulation results.

Based on this comparison, three model improvements to the network model are proposed. They concern the governing heat transfer correlation, the introduction of thermal boundary layer tracking and an improved description for the thermal resistance in the solid. The improved network model results in more accurate results.

INTRODUCTION

The thermal design of oil-cooled power transformer windings can be assessed by either CFD simulations or thermo-hydraulic network models. On the one hand, CFD simulations with commercial packages as performed by [2] are accurate, but time-consuming. On the other hand, thermo-hydraulic network models (THNM) have the advantage of low computational cost due to their use of essentially one-dimensional models. They describe the average oil velocity as well as oil and coil temperatures throughout the transformer windings, based on conservation laws and additional correlations for pressure drop and heat transfer. However, they crucially depend on the accuracy of the correlations in use.

There are several network models known in literature, e.g. [1], [3]–[5]. They are based on correlations described in literature [6], from experiments [7] or CFD simulations [8]. Our research concentrates on the specific situation in power transformers the correlations have to be valid for: laminar oil flow through channels a few millimetres wide.

This work aims at assessing and improving the thermal aspect of the network model of Radakovic & Sorgic [1]. The accuracy of the network model is assessed for a typical transformer winding configuration. It is validated against a CFD simulation. Next, several modelling improvements are introduced. Finally, the case study is executed again with these improvements.

NOMENCLATURE

A	[m²]	Area, width (L) times depth
D_h	[m]	Hydraulic diameter
d	[m]	Thickness
k	[W/mK]	Thermal conductivity
L	[m]	Width
l	[-]	Index running over all conductors
Nu	[-]	Nusselt number
Pr	[-]	Prandtl number of oil
q	[W/m^2]	Heat flux
Q	[W]	Heat
R	[K/W]	Thermal resistance
R_{1D}	[K/W]	1-dimensional thermal resistance
R_S	[K/W]	Spreading resistance
Re	[-]	Reynolds number
T	[K]	Temperature
x	[m]	Heated length
x^*	[-]	Dimensionless distance, defined in Eq. (5)

Special characters

Δq	[W/m^2]	Heat flux step
ΔT	[K]	Temperature difference
ε	[-]	Relative contact width
ξ	[-]	Dimensionless coordinate
θ	[-]	Dimensionless temperature

Subscripts

b	Bottom wall surface (temperature)
c	Copper
$conv$	Convective
$cond$	Conductive
e	Entry or inlet (temperature)
m	mean (temperature)
p	Paper
t	Top wall surface (temperature)

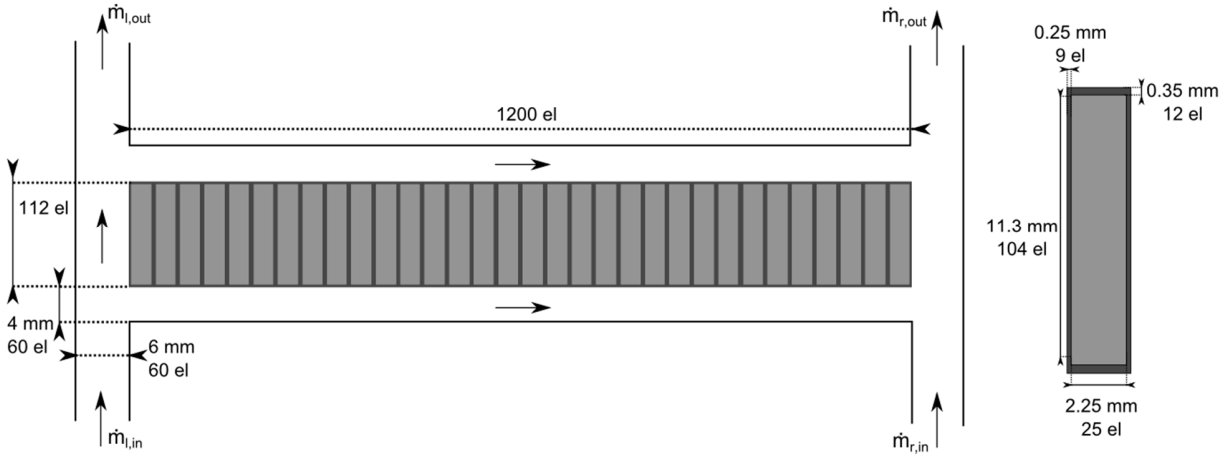

Fig. 1 Geometry under consideration: one disk, immersed in a net oil flow directed from left to right (left)(dark area is paper, lighter area is copper); detail of conductor (right). The mesh size for the CFD simulation is indicated by the number of elements (shortened el).

NETWORK MODEL ASSESSMENT

This section assesses the current accuracy of the network model for a typical transformer winding configuration.

Case study description

The case study comprises one disk of a larger disk winding, as depicted in Fig. 1. The disk is cooled by a net oil flow from left to right. Although the winding is rotationally periodic in reality, the geometry is assumed planar.

The disk is composed of 32 conductors. The conductors consist of copper surrounded by paper insulation. In this case, the insulation between conductors is thicker than the insulation between copper and oil, because the conductors are twin conductors. The copper has a thermal conductivity of 387.6 W/mK, whereas its value for the paper amounts to 0.16 W/mK. The loss density of the copper is 397.741 W/m³.

Hydrodynamically fully developed flow is imposed at both inlets with mass flows of 1.458 kg/s and 1.238 kg/s for the left and the right inlet respectively. The temperature at both sides is 310 K. The mass flow rates through the outlets are fixed at 1.005 kg/s and 1.691 kg/s, respectively for the left and the right outlet. The oil has a density of 868.89 kg/m³,

a dynamic viscosity of 0.0095 kg/ms and a thermal conductivity of 0.1307 W/mK. The properties are taken temperature independent, since their variation is very small over the considered domain. The largest Reynolds number is 355.6 (at the right outlet), which is still in the laminar flow regime. The cooling of the winding is oil-directed (OD), governed by forced convection.

CFD simulation

The geometry is meshed with Ansys ICEM and consists of a multi-block mesh with 170,000 elements. The mesh size in each direction for individual regions is indicated in Fig. 1.Where relevant, a non-uniform mesh has been applied. For example, the height of the first cell in the channels is 0.02 mm. A non-conformal mesh interface is defined between the fluid and the solid.

Ansys Fluent is used to solve the problem. A second order upwind scheme is applied to the convective terms, and a second order central scheme to the diffusive terms. The convergence criteria are set at 10^{-7} for the continuity equation and 10^{-12} for the energy equation. The global mass imbalance proves to be 4.93 10^{-13} kg/s. A mesh independence study with 2 times the number of elements of the original mesh shows variations of maximally 0.02 K on the temperature per conductor. Coarsening the mesh with a factor 2/3 resulted in differences of one order of magnitude higher, with a maximum of 0.2 K. The resulting number of cells quantitatively agrees well with the mesh of [2].

Network model

The network model of [1] is taken as a starting point for this study. Its use is limited to the module for the simulation of the winding. As the flow is imposed, only the thermal component of this model is relevant. The disk and the surrounding oil take part in a thermal network, of which the temperature nodes are displayed in Fig. 2. Between temperature nodes, there is a thermal resistance. The heat transfer is governed by:

$$Q = \frac{\Delta T}{R_{total}} = \frac{\Delta T}{R_{cond}+R_{conv}} \quad (1)$$

Where q is the heat flux, ΔT the temperature difference and R the thermal resistance. The thermal resistances are shown on Fig. 2. Between the centre of the copper and the surface of the paper is a conductive resistance, which is governed by Fourier's law. In Radakovic & Sorgic' model it is determined with:

$$R_{cond} = \frac{d_p}{k_p A_c} \tag{2}$$

with A the 'top' area of the copper, i.e. width times depth. The convective resistance between paper and oil is determined by a convection coefficient, which is determined by a correlation from Hausen [9].

$$Nu_D = 3.66 + \frac{0.0668\, D/L\, Re_D Pr}{1+0.04(D/L Re_D Pr)^{2/3}} \tag{3}$$

which is valid for laminar, thermally developing flow in circular tubes with constant surface temperature.

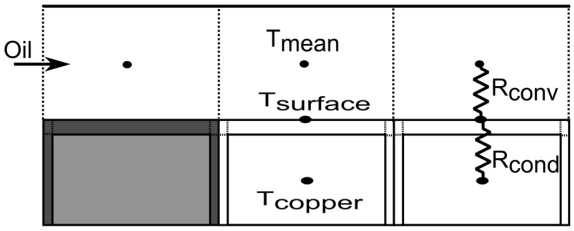

Fig. 2: Nodes in the network model. The arrow indicates the oil flow direction (dark area is insulation paper, lighter area is copper)

Results

The obtained conductor temperatures with CFD and THNM are displayed in Fig. 3. The network model generally overestimates the conductor temperatures. Only at the right side of the disk, the temperature is lower than those of the CFD simulation. These observations are also reflected by the relevant characteristic quantities summarised in Table 1. The characteristic temperatures are the mean winding temperature $\overline{T}_c$ and the hot-spot temperature.

Table 1: Characteristic temperatures.

	$\overline{T}_c$ [K]	max(T_c) [K]
CFD	319.98	322.1
Radakovic & Sorgic	322.49	323.8

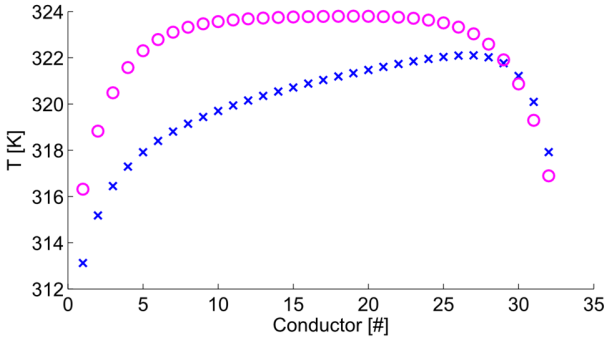

Fig. 3: Temperature of each conductor, numbered from left to right (crosses for CFD results, circles for THNM)

MODEL IMPROVEMENTS

This section details the changes proposed with respect to the original model of [1].

Heat transfer correlation

The heat transfer correlation for the Nusselt number is replaced by [6]:

$$Nu_x = \frac{h D_h}{k} = \left[\frac{17}{140} + \frac{1}{4}\sum_{n=1}^{\infty} C_n Y_n(1)\exp(-32/3\,\beta_n^2 x^*)\right]^{-1} \tag{4}$$

This correlation is valid for hydraulically fully developed flow and thermally developing flow between parallel plates. The thermal boundary conditions are two-side heated constant heat flux conditions. The terms C_n, $Y_n(1)$ and β_n are constants, eigenfunctions and eigenvalues, respectively. They are further detailed in Shah and London [6]. The dependent variable is the dimensionless distance:

$$x^* = \frac{x/D_h}{RePr} \tag{5}$$

With x is the heated length, D_h the hydraulic diameter, Re the Reynolds number and Pr the Prandtl number of the oil.

The correlation can also be used for one-side heated problems by filling in the appropriate values from [10]. This paves the way for the application of the superposition technique.

The influence of both walls on the surface temperature is:

$$T_t = \frac{D_h}{k}(q_t\theta_{tt} + q_b\theta_{tb}) + T_e \tag{6}$$

with T_t the top wall surface temperature, q the heat flux [W/m²], θ the dimensionless temperature and T_e the inlet temperature. The subscripts b and t refer to the bottom and top wall, respectively. The dimensionless temperature of the top wall is:

$$\theta_{tt} = \frac{T_t - T_e}{q_t \frac{D_h}{k}} = 2x^* + 0.185714 + \sum_{n=1}^{\infty} C_{nt} Y_n(1) \exp(-{}^{32}/_{3}\, \beta_n^2 x^*) \quad (7)$$

$$\theta_{tb} = \frac{T_t - T_e}{q_t\, D_h/k} = 2x^* - 0.0642857 + \sum_{n=1}^{\infty} C_{nb} Y_n(1) \exp(-{}^{32}/_{3}\, \beta_n^2 x^*) \quad (8)$$

where the values for $C_n Y_n(1)$ at top and bottom have the same magnitude, with positive values for odd values of n in the bottom case, and negative values in all other cases. The bottom wall surface temperature can be obtained by interchanging the indices b and t.

The calculation of the mean temperature T_m is similar to (6), but now expressed in terms of the dimensionless mean temperature:

$$\theta_{m,t} = \frac{T_m - T_e}{q_t\, D_h/k} = 2x^* \qquad \theta_{m,b} = \frac{T_m - T_e}{q_b\, D_h/k} = 2x^* \quad (9)$$

Superposition is applied in the direction along the flow: the wall temperature is given by:

$$T_t = T_m + \sum_l \left(\frac{\Delta q_t\, D_h}{k}\right)_l [\theta_{tt}(x^* - \xi_l) - \theta_{mt}(x^* - \xi_l)] + \sum_l \left(\frac{\Delta q_b\, D_h}{k}\right)_l [\theta_{tb}(x^* - \xi_l) - \theta_{mb}(x^* - \xi_l)] \quad (10)$$

Where ξ is the dimensionless coordinate at which the flux changes and Δq the change in the flux. In the case of the network model, we will model the flux profile as a block flux, i.e. the flux is constant along each conductor element.

The use of the correlation has to be adapted in the context of the network model. The network model only contains one node per conductor, as depicted in Fig. 2. In order to calculate a meaningful value of the convection coefficient, the following formula is applied:

$$Nu_l = \frac{1}{L_p} \int_{x=(l-1)L_p}^{x=l\,L_p} Nu_x dx \quad (11)$$

With l the index corresponding to the conductor number (starting from 1, as in Eq. (10)), and L_p the width of the paper (equal to the width of the conductor).

Thermal boundary layer

The thermal boundary layer developing at the most left conductor in the vertical channel is convected into the upper channel. Similarly, the thermal boundary layer growing along the bottom of the conductors and is convected into the right vertical channel. This continuation has to be reflected in the correlations:

$$x^*_{cont} = \frac{(x + x_{prev})/D_h}{Re\ Pr} \quad (12)$$

Where x_{prev} is the distance [m] over which the thermal boundary has already been developed. Notice that the hydraulic diameter and the Reynolds number change after the junction.

It should be noted that it is possible a recirculation region develops after the corner. This affects the surface temperature of the underlying conductors, but results in a local effect only: the boundary layer thickness is largely unaffected.

Spreading resistance

The total resistance is the sum of conductive and convective resistances. The spreading resistance is added to the 1-dimensional resistance [11]:

$$R_{total} = R_s + R_{1D} = R_s + \frac{d_p}{k_p\, A_p} + \frac{1}{h\, A_p} \quad (13)$$

Where the copper is represented as a heat source with a certain flux distribution. The expression for the spreading resistance is [11]:

$$k_p R_s = \frac{1}{\pi^2\, \epsilon} \sum_{n=1}^{\infty} \frac{sin(n\pi\epsilon)\, J_0(n\pi\epsilon)}{n^2} \quad (14)$$

with ϵ the relative contact width, i.e. the width of the copper on the width of the conductor and J_0 the Bessel function of the first kind of order 0. This expression is valid for an equivalent isothermal flux distribution.

RESULTS WITH IMPROVED MODELLING

The network model is now evaluated with the improvements from section 3 incorporated. The resulting temperature distribution is presented in Fig. 4. The predicted temperature of the copper is slightly lower than the temperature of the CFD simulation. This is reflected by the mean copper temperature and

the hot-spot temperature, which are respectively 319.6 K and 321.8 K. This means that the deviation of the network model from the CFD simulation has lowered from 2.5 K to 0.4 K for the mean copper temperature and 1.7 K to 0.3 K for the hot-spot temperature. Furthermore, the temperature profile well resolved.

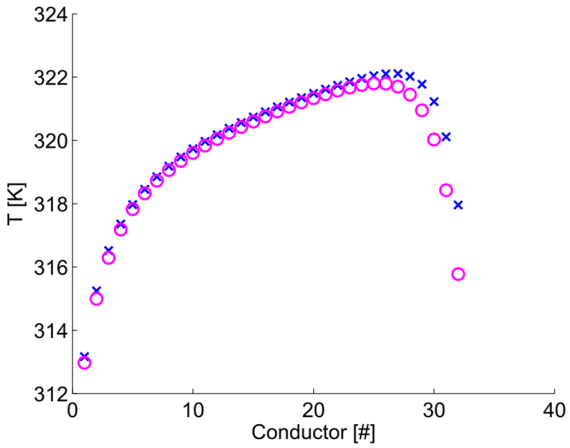

Fig. 4: Temperature of each conductor, numbered from left to right (crosses for CFD results, circles for the improved THNM)

A minor difference between the calculations still exists. The largest deviation is now situated at the right side of the disk. From comparison with the more accurate CFD results this difference can be attributed to the velocity profile in the outer axial channel, which is drawn in

Fig. 5. This is induced by the flow from the lower horizontal channel entering the vertical channel which pushes the latter to the right. As a result the velocity gradient at the disk surface is lower than the one obtained from a parabolic velocity profile. This lowers the convection coefficient and increases disk temperature. This effect is not included in the network model.

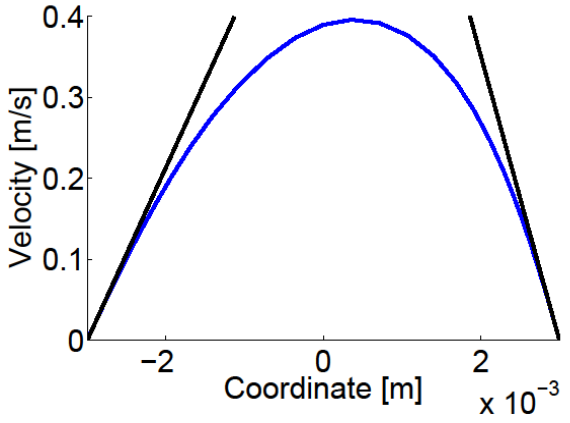

Fig. 5: Velocity profile in the right vertical channel at half-conductor height.

CONCLUSION

In this paper the heat transfer from the conductors in a power transformer winding to the cooling oil is studied. Results of the network model by [1] is assessed using the results of a CFD simulation. The temperatures of the conductors predicted by the network model were generally too high. Therefore, three aspects of the network model were changed: the heat transfer correlation, the way of tracking the thermal boundary layer and the thermal resistance between copper and oil. These improvements led to network model results that are more accurate: differences of winding temperatures compared with the CFD reference results are on averaged lowered with a factor 6. The remaining discrepancy can be attributed to the shape of the velocity profile due to bending flow around the lower right corner.

Acknowledgements

The authors acknowledge support from the IWT, in the context of a Baekeland Mandate.

REFERENCES

[1] Z. R. Radakovic and M. S. Sorgic, “Basics of Detailed Thermal-Hydraulic Model for Thermal Design of Oil Power Transformers,” *IEEE Trans. Power Deliv.*, vol. 25, no. 2, pp. 790–802, Apr. 2010.

[2] F. Torriano, M. Chaaban, and P. Picher, “Numerical study of parameters affecting the temperature distribution in a disc-type transformer winding,” *Appl. Therm. Eng.*, vol. 30, no. 14–15, pp. 2034–2044, Oct. 2010.

[3] A. J. Oliver, “Estimation of transformer winding temperatures and coolant flows using a general network method,” *IEE Proc. C Gener. Transm. Distrib.*, vol. 127, no. 6, pp. 395–405, 1980.

[4] R. M. Del Vecchio and P. Feghali, “Thermal model of a disk coil with directed oil flow,” in *IEEE Transmission and Distribution Conference*, 1999, vol. 2, pp. 914–919.

[5] J. Zhang and X. Li, “Oil Cooling for Disk-Type Transformer Windings—Part II:

Parametric Studies of Design Parameters," *IEEE Trans. Power Deliv.*, vol. 21, no. 3, pp. 1326–1332, Jul. 2006.

[6] R. K. Shah and A. L. London, *Laminar Flow Forced Convection in Ducts*. Elsevier, 1978.

[7] J. Zhang, X. Li, and M. Vance, "Experiments and modeling of heat transfer in oil transformer winding with zigzag cooling ducts," *Appl. Therm. Eng.*, vol. 28, no. 1, pp. 36–48, Jan. 2008.

[8] W. Wu, Z. D. Wang, A. Revell, H. Iacovides, and P. Jarman, "Computational fluid dynamics calibration for network modelling of transformer cooling oil flows-part I heat transfer in oil ducts," *Iet Electr. Power Appl.*, vol. 6, no. 1, pp. 19–27, 2012.

[9] F. P. Incropera and D. P. DeWitte, *Fundamentals of Heat and Mass Transfer*, 5th ed. John Wiley & Sons, 2002.

[10] R. Lundberg, W. Reynolds, and W. Kays, "Heat transfer with laminar flow in concentric annuli with constant and variable wall temperature and heat flux," 1961.

[11] M. M. Yovanovich, Y. S. Muzychka, and J. R. Culham, "Spreading resistance of isoflux rectangles and strips on compound flux channels," *J. Thermophys. Heat Transf.*, vol. 13, no. 4, 1999.